



Deposited via The University of Leeds.

White Rose Research Online URL for this paper:

<https://eprints.whiterose.ac.uk/id/eprint/155105/>

Version: Accepted Version

Article:

Chu, F, Gao, S, Zhang, X et al. (2019) Droplet re-icing characteristics on a superhydrophobic surface. *Applied Physics Letters*, 115 (7). 073703. ISSN: 0003-6951

<https://doi.org/10.1063/1.5109283>

© 2019 Author(s). This article may be downloaded for personal use only. Any other use requires prior permission of the author and AIP Publishing. The following article appeared in Chu, F, Gao, S, Zhang, X et al. (2 more authors) (2019) Droplet re-icing characteristics on a superhydrophobic surface. *Applied Physics Letters*, 115 (7). 073703. ISSN 0003-6951, and may be found at <https://doi.org/10.1063/1.5109283>. Uploaded in accordance with the publisher's self-archiving policy.

Reuse

Items deposited in White Rose Research Online are protected by copyright, with all rights reserved unless indicated otherwise. They may be downloaded and/or printed for private study, or other acts as permitted by national copyright laws. The publisher or other rights holders may allow further reproduction and re-use of the full text version. This is indicated by the licence information on the White Rose Research Online record for the item.

Takedown

If you consider content in White Rose Research Online to be in breach of UK law, please notify us by emailing eprints@whiterose.ac.uk including the URL of the record and the reason for the withdrawal request.

Droplet re-icing characteristics on a superhydrophobic surface

Fuqiang Chu,¹ Sihang Gao,² Xuan Zhang,² Xiaomin Wu,² and Dongsheng Wen^{1,3, a)}

¹*School of Aeronautic Science and Engineering, Beihang University, Beijing 100191, China*

²*Department of Energy and Power Engineering, Tsinghua University, Beijing 100084, China*

³*School of Chemical and Process Engineering, University of Leeds, Leeds LS2 9JT, UK*

a) Author to whom correspondence should be addressed; E-mail: d.wen@buaa.edu.cn

Abstract

Water icing is a natural phase change phenomenon which happens frequently in nature and industry and has negative effects on a variety of applications. Deicing is essential for iced surfaces, but even for a nanoengineered superhydrophobic surface, deicing may be incomplete with many adherent unmelted ice droplets which have potential of re-icing. Here, we focused on the droplet re-icing characteristics on a solid superhydrophobic surface, which has lacked attention in previous studies. Our results show that, the nucleation and ice crystal growth characteristics of a re-icing droplet are quite different with those of a first-time icing droplet. During re-icing, secondary nucleation due to fluid shear always first occurs on the edges of unmelted ice, accompanied by fast-growing ice crystals that can trigger heterogeneous nucleation when in contact with the solid surface. The re-icing takes place under very small supercooling (less than 0.5°C) and the superhydrophobic surface does not play a key role, meaning that any current icephobic surfaces lose their features, which poses great challenges for anti-icing. In addition, because of the small supercooling, no recalescence phenomenon appears during re-icing and the droplet keeps transparent instead of clouding. Owing to the unmelted ice floating on the top of the droplet, the droplet shape after re-icing is also distinguishing from that after normal icing but the pointy tip formation during re-icing and normal icing shows a uniformity. These results shall deepen the understanding on the anti-icing and deicing physics.

Main Text

Icing phenomenon is ubiquitous in nature and industry. When the ambient temperature is below the freezing point, a water droplet freezes. In most instances, icing is undesired and has adverse effects on a variety of human activities, such as reduces the crop production in agriculture,¹ threatens the flight safety in aviation,² and deteriorates the heat transfer in heat exchanger systems.³ Thus, to avoid the hazards of icing, icing mechanisms and anti-icing technologies have received considerable attentions over the past decades. Researchers have figured out the ice nucleation physics (homogeneous nucleation at liquid-air interface or heterogeneous nucleation at solid-liquid interface) under humidity or gas flow environments,⁴⁻⁶ investigated the freezing front growth and droplet shape evolution features,^{7,8} and revealed the pointy tip formation mechanism at the later stage of icing.^{9,10} Besides basic studies on icing, many anti-icing methods are proposed to suppress the ice accretion, one of which is the application of nanoengineered surfaces.^{11,12} Researchers fabricated numerous surfaces with various structures and wettability with the purpose of delaying the ice nucleation,¹³⁻¹⁵ retarding the ice propagation,^{16,17} reducing the ice adhesion,^{18,19} and even self-cleaning subcooled droplets or melting frost by a kind of self-jumping behavior,²⁰⁻²⁵ and have achieved expected results.

Since a nanoengineered surface cannot inhibit icing completely,^{11,26} deicing is essential.²⁷ In practical applications, deicing may be incomplete with many water or ice-water mixed droplets adhering to the surface.^{17,24} These residual, unmelted droplets will freeze again when the surface temperature decreases below 0°C in the next operation cycle of equipment. However, research on the icing characteristics of an unmelted, ice-water mixed droplet (we call it re-icing here) on solid surfaces is quite rare, while the re-icing of a droplet is subsistent in practice and worthy of intensive concern. In the present work, we conducted re-icing experiments by refreezing a melting droplet again, and investigated the nucleation and ice crystal growth characteristics of the re-icing droplet,

which is quite different with those characteristics of a normal icing droplet. We also found that the ice droplet shape and the pointy tip size at the top of the ice droplet after re-icing is distinguishing from those after normal icing. We expect that this work could bring insight into anti-icing and deicing mechanisms and applications.

In the experiments, an Al-based surface fabricated by the chemical etching–deposition method²⁸ was used as the experimental surface. At room temperature (20°C), the experimental surface is superhydrophobic with a contact angle (CA) of $159.1\pm 1.6^\circ$ (the standard deviations of the CA measurements are based on five measurements), but when the test droplet was deposited on a supercooled surface (-20°C), its CA gradually decreased to $147.2\pm 1.2^\circ$. This is mainly due to the capillary condensation and thin water film formation adjacent to the triple phase line.²⁹ The decreasing of the droplet CA on a supercooled surface also indicates a wetting transition from Cassie-Baxter state to Wenzel state. See supplementary material S2 for more information about the experimental surface and the contact angle measurement. In the re-icing experiments, we located millimeter sessile droplets (deionized water) on the experimental surface, and then reduced the surface temperature to -20°C \sim -15°C to cool the droplet and make it icing. After the droplet was frozen completely, the surface temperature was increased by controlling the voltage of the thermoelectric cooler. When the droplet temperature rose above 0°C , the ice droplet began to melt. Before the droplet melted completely, the surface temperature was reduced below 0°C again to re-cool the droplet, and the unmelted droplet (composed of ice and water) was re-frozen. This is the experimental procedure of re-icing. During the experiments, the lab temperature was measured to be $20.0\pm 1.0^\circ\text{C}$ with a relative humidity range from 20% to 40%. Figure 1 draws the typical variations in the surface temperature and the droplet temperature during one experiment. It should be noted that we used T-type thermocouples (0.127 mm cable diameter with an accuracy of $\pm 0.5^\circ\text{C}$) to measure the surface and droplet temperature, and when measuring the droplet temperature, the thermocouples were inserted inside the droplet and located at the droplet center as much as possible. Since the inserted thermocouples may yield some influence on the droplet temperature, the droplet temperature variation measured by inserted thermocouples in Fig. 1 is not the precise temperature of the re-icing droplet without thermocouples (such as the one in Fig. 2). However, based on many times of repeated measurements, we demonstrated that the measured droplet temperature is representative and reliable for the re-icing process. See supplementary material S3 for more information about the experiments, including the experimental setup and the droplet temperature measurement.

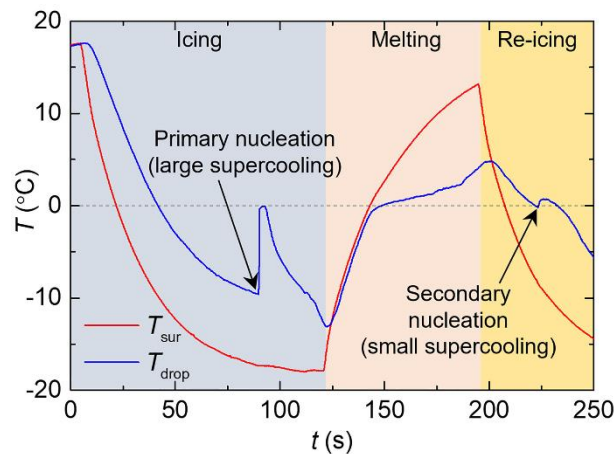


FIG. 1. Typical variations in the surface temperature and the droplet temperature during one re-icing experiment. During the whole experiment, firstly, normal icing occurs. Large supercooling degree is needed for the primary nucleation during normal icing, and recalescence happens after nucleation, making the droplet clouding, and the droplet temperature rises to 0°C after recalescence. Secondly, ice droplet melts. Thirdly, before the droplet finishes melting, the droplet is re-cooled and re-icing occurs. Due to the existence of unmelted ice in droplet, secondary nucleation occurs during re-icing under very small supercooling degree, and no clouding phenomenon appears during re-icing.

Figure 2 shows the side-view of a typical re-icing process of a droplet. In Fig. 2, the time when the ice droplet begins to melt is regarded as 0 s. During melting, the droplet temperature continues to increase and embedded bubbles in the ice are released and fast moving (See supplementary material S1 for multimedia evidences). The fast bubble moving behavior reflects severe internal thermocapillary convection which is caused by the temperature gradient inside the melting droplet. Via adding multiwall carbon nanotubes as trace particles, experiments by Ivall *et al.* also proved the thermocapillary convection inside a melting droplet.³⁰ Then, at appropriate time (28 s in Fig. 2), the surface temperature is reduced and the droplet is re-cooled. One can see the bubbles are dissolved into the water again due to the decreased droplet temperature. When the droplet temperature is slightly below 0°C with a small degree of supercooling, nucleation forms on the edge of the unmelted ice, stretching dendritic crystals (40.51~41.51 s). Considering the existence of unmelted ice and the internal convection inside the droplet, we conclude that the nucleation on the ice edge during re-icing is a kind of secondary nucleation and it is induced by fluid shear.^{31,32} During re-icing, the unmelted ice serves as an important resource of ice nuclei, and the fluid flow caused by temperature gradient could shear off many tiny ice particles from the unmelted ice (see supplementary material S4 for the experimental evidences), thus the ice nuclei concentration in liquid phase is increased, which enhances the secondary nucleation. The secondary nucleation is different from the primary nucleation (homogeneous or heterogeneous), it has lower nucleation energy barrier³³ and does not rely on large supercooling. According to our statistics based on multiple experimental tests, the average supercooling degree for the secondary nucleation during re-icing is 0.39°C with a deviation of 0.36°C.

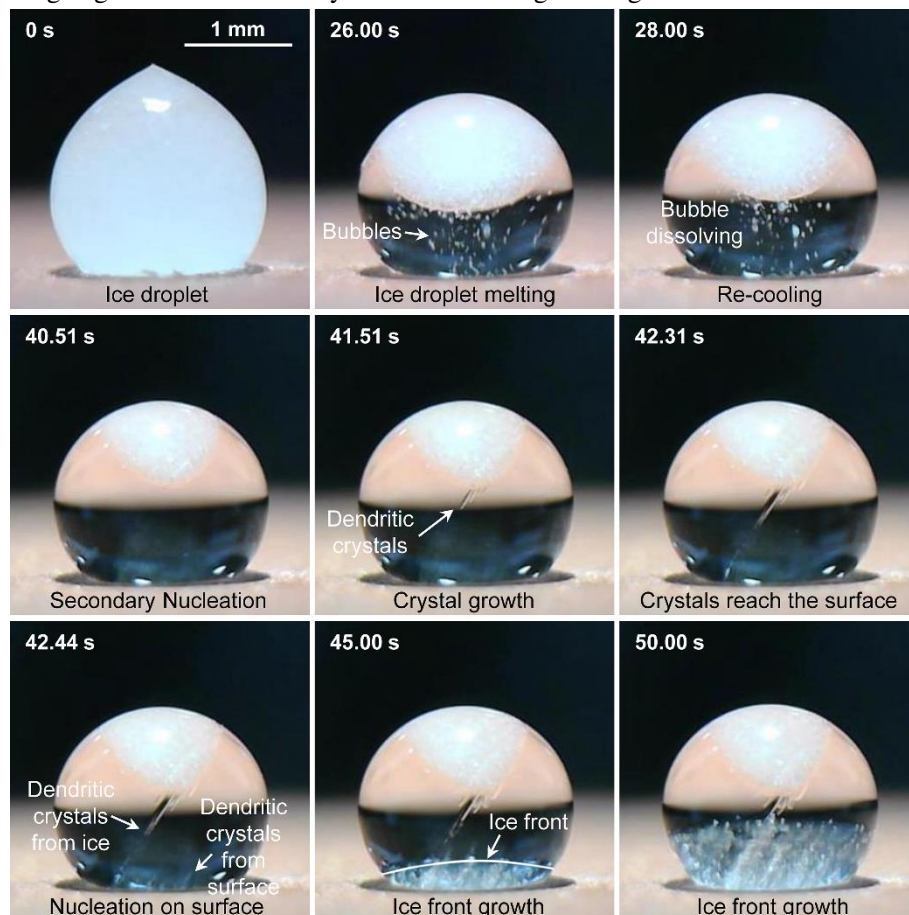


FIG. 2. Re-icing process of a 4 μL droplet (side-view). From 0 s to 28 s, the ice droplet melts and the embedded bubbles in ice are released. From 28 s to about 40 s, the droplet is re-cooled with these released air bubbles dissolved in water again. Then, when the droplet is re-cooled to a little below 0°C, secondary nucleation on the edge of unmelted ice occurs and dendritic crystals grow downwards from the ice, reach the superhydrophobic surface, and trigger extra heterogeneous nucleation and crystal growth on the surface (40.51~42.44 s). Thereafter, freezing starts and the ice front moves upwards until the droplet finishes freezing. Multimedia view: [URL]

Once the secondary nucleation starts, ice dendritic crystals grow from the unmelted ice very rapidly, reaching the solid superhydrophobic surface in millisecond (41.51~42.31 s), and the touching of dendritic crystals will trigger extra heterogeneous nucleation on the surface. As shown in Fig. 2 near 42.44 s, one can see ice dendritic crystal growth from the surface. During this stage of nucleation and rapid ice crystal growth, the droplet temperature rises above 0°C a little due to the small amounts of releasing latent heat. Thereafter, freezing stage starts and the ice front grows upwards from the solid superhydrophobic surface until the droplet is frozen completely. See supplementary material S1 for multimedia which shows the whole re-icing process more clearly. Supplementary material S5 also shows a re-icing case from top-view.

The normal icing of a droplet usually experiences two stages including nucleation/recalescence and freezing, where the former is a very rapid, kinetically controlled process, and the latter is a heat transfer controlled process.⁴ We also divided the re-icing process into two stages, *i.e.*, the nucleation stage and the freezing stage. However, the first stage of re-icing is quite different with that of normal icing, as shown in Fig. 3. In the nucleation stage of re-icing, secondary nucleation due to fluid shear on the edge of unmelted ice first occurs, which is accompanied by rapid dendritic crystal growth from the unmelted ice. When these crystals touch the solid superhydrophobic surface, they trigger extra heterogeneous nucleation on the surface.

One may notice that the droplet keeps limpid during re-icing without the common clouding phenomenon appearing. This is because the secondary nucleation occurs under very small supercooling degree ($0.39\pm 0.36^\circ\text{C}$). One can calculate the ice crystal fraction during nucleation in the liquid part of the droplet based on,^{5,34}

$$f_{\text{crystal}} = \frac{Cp\Delta T}{L} \quad (1)$$

where f_{crystal} is the ice crystal fraction in the liquid part of the droplet during the secondary nucleation; Cp is the heat capacity of water; L is the latent heat of solidification of water; ΔT is the supercooling degree. According to above formula, the calculated ice crystal fraction is only $0.50\pm 0.46\%$. Such little ice crystal is not enough to cause the droplet to be clouding. And because the re-icing droplet is transparent, the bubble formation on the ice front is very clear, which is reported in our another work (See supplementary material S5 for clear bubble formation in re-icing droplets).³⁵ In addition, because the re-icing starts from the secondary nucleation on unmelted ice, any current icephobic surfaces,^{11,36,37} such as a nanoengineered superhydrophobic surface, lose their anti-icing properties. This do limit the development of anti-icing applications and bring some challenges.

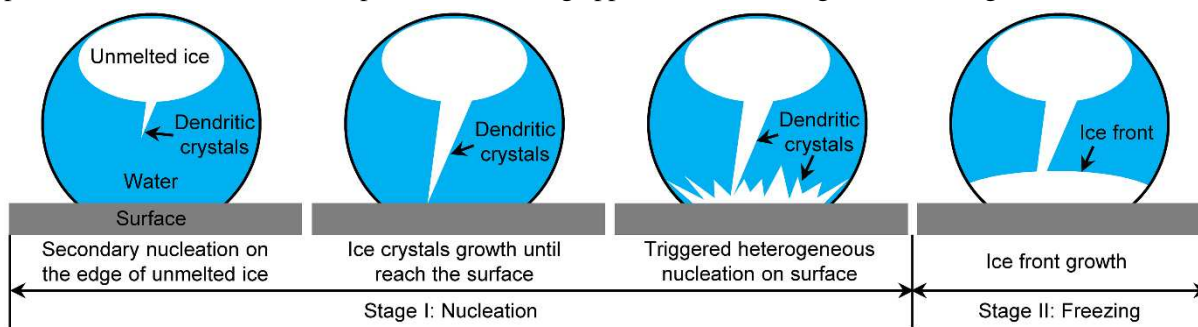


FIG. 3. Schematic of re-icing process. Two stages are divided including the nucleation stage and the freezing stage.

In the first stage, secondary nucleation first occurs on the edge of unmelted ice, along with dendritic crystal stretching from the unmelted ice. When these ice crystals reach the solid surface, they trigger heterogeneous nucleation on the surface.

Besides the nucleation and ice crystal growth characteristics, the ice droplet shape after re-icing is also distinguishing from those after normal icing. As the example (1 μL droplet) in Fig. 4(a) shown, the re-icing droplet is more spherical with a shorter height and a smaller tip (See supplementary material S6 for more re-icing droplet examples). This is because the unmelted ice floating on the top of the droplet serves as a framework,

which immobilizes the upper part of the droplet and limits the premature formation of pointy tip. But the pointy tip forms during re-icing finally. Figure 4(b) shows the schematic of tip formation in the re-icing process. When ice melts, the ice is covered by a thin water layer,³⁸ and when the ice front passes the unmelted ice during re-icing, the ice front actually moves in the thin water layer, producing a very tiny water pool at the later stage of re-icing. Due to the density difference between water and ice, the freezing of the tiny water pool results in a tiny tip at the top of the re-icing droplet.

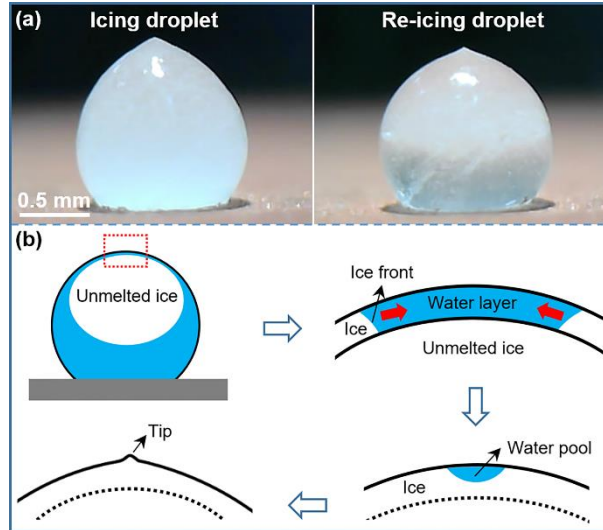


FIG. 4. (a) Comparison of droplet shape after normal icing and re-icing (1 μL droplet). The re-icing droplet is closer to a sphere with a shorter height and a smaller tip. (b) Schematic of tip formation in the re-icing process.

The unmelted ice is covered by a thin water layer, and the ice front moves in the water layer during re-icing, producing a tiny water pool. Similar with the tip formation during normal icing, freezing of this water pool also forms a tip, but this tip is much smaller.

We also measured the tip angles during re-icing for various droplet volumes (from 2 to 10 μL), and compared them with those tip angles during normal icing, as shown in Fig. 5(a). Consistent with previous research,¹⁰ the average tip angle of icing droplets is measured to be 127.0° with a deviation of 4.4° . The average tip angle of re-icing droplets is $128.1 \pm 4.9^\circ$, which is almost indistinguishable from the former. All the tip angles are located in the range of $120\text{-}140^\circ$. We also drew the relationship between the tip angle and the droplet volume for both icing droplets and re-icing droplets in Fig. 5(b), but the results show that the two parameters seem to have no certain relationship. Marin *et al.* concluded that the tip angle is independent of substrate temperature and wetting angle, they suggested a universal, self-similar mechanism of tip formation that does not depend on the rate of solidification.⁹ Our experiments also suggest that, for both re-icing and icing droplets, though the tip sizes are different, the tip angles have a similarity, and are independent of droplet volume.

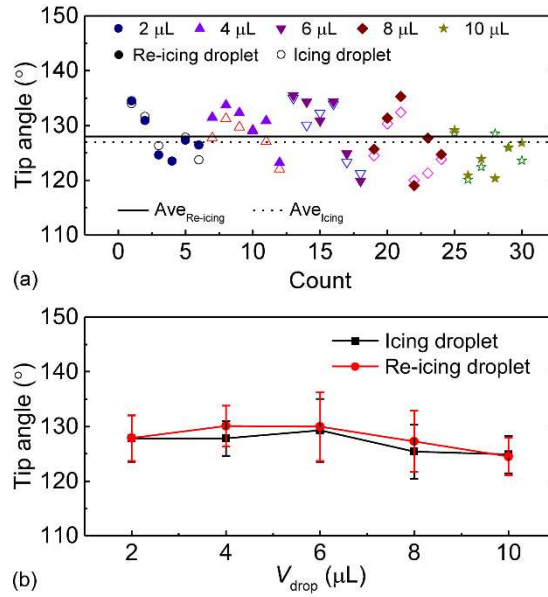


FIG. 5. (a) Tip angles of icing droplets and re-icing droplets with various droplet volumes. All the tip angles are located in the range of 120-140°, which is consistent with previous studies. The average tip angle of icing droplet is 127.0° with a deviation of 4.4°, and the value for re-icing droplets is 128.1±4.9°. (b) Relationship between tip angle and droplet volume for both icing droplets and re-icing droplets. The experiments suggest that the tip angle is independent of droplet volume.

In summary, re-icing characteristics of an unmelted droplet (ice-water mixture) located on a solid superhydrophobic surface were investigated in this letter. Similar with normal droplet icing, the re-icing process also contains two stages including the nucleation stage and the freezing stage. But the nucleation stage of re-icing is quite different with that of normal icing. The first difference is that secondary nucleation induced by fluid shear always first occurs on the edge of unmelted ice during re-icing. As a result, the influence of solid surface property is excluded and any anti-icing surfaces lose their nucleation delay features. The second difference is that the ice crystal fraction during nucleation in the liquid part of a re-icing droplet is so small that the re-icing droplet keeps transparent instead of clouding. In addition, owing to the unmelted ice cover, the droplet shape and the pointy tip size after re-icing are also distinguishing from those after normal icing, but the tip angle of a re-icing droplet has no obvious difference with that of a normal ice droplet. We expect that this work could deepen our understanding on icing physics and bring inspirations for anti-icing technology.

Supplementary Material

See supplementary material for more details about the experiments and more images of the re-icing process.

Acknowledgments

This work is supported by the National Postdoctoral Program for Innovative Talents (No. BX20180024) and the China Postdoctoral Science Foundation (No. 2019M650444).

- 1 M. P. Fuller, A. M. Fuller, S. Kaniouras, J. Christophers, and T. Fredericks, *Eur. J. Agron.* 26 (4), 435 (2007).
- 2 F. T. Lynch and A. Khodadoust, *Prog. Aerospace Sci.* 37, 669 (2001).
- 3 M. R. Nasr, M. Fauchoux, R. W. Besant, and C. J. Simonson, *Renewable Sustainable Energy Rev.* 30, 538 (2014).
- 4 S. Jung, M. K. Tiwari, N. V. Doan, and D. Poulidakos, *Nat. Commun.* 3, 615 (2012).
- 5 M. Schremb and C. Tropea, *Phys. Rev. E* 94, 052804 (2016).
- 6 P. Hao, C. Lv, and X. Zhang, *Appl. Phys. Lett.* 104 (16), 161609 (2014).

- 7 M. Tembely and A. Dolatabadi, *J. Fluid Mech.* 859, 566 (2018).
- 8 X. Zhang, X. Liu, J. Min, and X. Wu, *Appl. Therm. Eng.* 147, 927 (2019).
- 9 A. G. Marin, O. R. Enriquez, P. Brunet, P. Colinet, and J. H. Snoeijer, *Phys. Rev. Lett.* 113, 054301 (2014).
- 10 M. F. Ismail and P. R. Waghmare, *Appl. Phys. Lett.* 109, 234105 (2016).
- 11 T. M. Schutzius, S. Jung, T. Maitra, P. Eberle, C. Antonini, C. Stamatopoulos, and D. Poulikakos, *Langmuir* 31, 4807 (2015).
- 12 L. Oberli, D. Caruso, C. Hall, M. Fabretto, P. J. Murphy, and D. Evans, *Adv. Colloid Interface Sci.* 210, 47 (2014).
- 13 Y. Hou, M. Yu, Y. Shang, P. Zhou, R. Song, X. Xu, X. Chen, Z. Wang, and S. Yao, *Phys. Rev. Lett.* 120, 075902 (2018).
- 14 X. Sun and K. Rykaczewski, *ACS Nano* 11 (1), 906 (2017).
- 15 J. L. O'Brien, S. F. Ahmadi, K. C. Failor, C. E. Bisbano, M. D. Mulroe, S. Nath, B. A. Vinatzer, and J. B. Boreyko, *Appl. Phys. Lett.* 113 (15), 153701 (2018).
- 16 Y. Zhao and C. Yang, *Appl. Phys. Lett.* 108 (6), 061605 (2016).
- 17 F. Chu, X. Wu, and L. Wang, *ACS Appl. Mater. Interfaces* 9, 8420 (2017).
- 18 K. Golovin, S. P. Kobaku, D. H. Lee, E. T. DiLoreto, J. M. Mabry, and A. Tuteja, *Sci. Adv.* 2 (3), e1501496 (2016).
- 19 M. J. Nine, T. T. Tung, F. Alotaibi, D. N. Tran, and D. Losic, *ACS Appl. Mater. Interfaces* 9 (9), 8393 (2017).
- 20 F. Chu, X. Wu, B. Zhu, and X. Zhang, *Appl. Phys. Lett.* 108 (19), 194103 (2016).
- 21 Y. Cheng, B. Du, K. Wang, Y. Chen, Z. Lan, Z. Wang, and X. Ma, *Appl. Phys. Lett.* 114 (9), 093704 (2019).
- 22 J. B. Boreyko and C. P. Collier, *ACS Nano* 7 (2), 1618 (2013).
- 23 Q. Zhang, M. He, J. Chen, J. Wang, Y. Song, and L. Jiang, *Chem. Commun.* 49 (40), 4516 (2013).
- 24 F. Chu, D. Wen, and X. Wu, *Langmuir* 34 (48), 14562 (2018).
- 25 Y. Shen, M. Jin, X. Wu, J. Tao, X. Luo, H. Chen, Y. Lu, and Y. Xie, *Appl. Therm. Eng.* 156, 111 (2019).
- 26 K. K. Varanasi, T. Deng, J. D. Smith, M. Hsu, and N. Bhate, *Appl. Phys. Lett.* 97 (23), 234102 (2010).
- 27 K. Golovin, A. Dhyani, M. D. Thouless, and A. Tuteja, *Science* 364 (6438), 371 (2019).
- 28 F. Chu and X. Wu, *Appl. Surf. Sci.* 371, 322 (2016).
- 29 F. Tavakoli and H. P. Kavehpour, *Langmuir* 31 (7), 2120 (2015).
- 30 J. Ivall, J. Renault-Crispo, S. Coulombe, and P. Servio, *Int. J. Heat Mass Transfer* 101, 27 (2016).
- 31 G. D. Botsaris, in *Industrial Crystallization*, edited by J. W. Mullin (Springer US, Boston, MA, 1976), pp. 3.
- 32 S. G. Agrawal and A. H. J. Paterson, *Chem. Eng. Commun.* 202 (5), 698 (2015).
- 33 S. I. A. Cohen, R. Cukalevski, T. C. T. Michaels, A. Saric, M. Tornquist, M. Vendruscolo, C. M. Dobson, A. K. Buell, T. P. J. Knowles, and S. Linse, *Nat. Chem.* 10 (5), 523 (2018).
- 34 L. Makkonen, *Appl. Phys. Lett.* 96 (9), 091910 (2010).
- 35 F. Chu, X. Zhang, S. Li, H. Jin, J. Zhang, X. Wu, and D. Wen, *Phys. Rev. Fluids* (2019).
- 36 P. Tourkine, M. Le Merrer, and D. Quere, *Langmuir* 25 (13), 7214 (2009).
- 37 L. Mishchenko, M. Khan, J. Aizenberg, and B. D. Hatton, *Adv. Funct. Mater.* 23 (36), 4577 (2013).
- 38 J. G. Dash, *Science* 246, 1591 (1989).